Biochimica et Biophysica Acta 1838 (2014) 988–993

Contents lists available at ScienceDirect

Biochimica et Biophysica Acta

journal homepage: www.elsevier.com/locate/bbamem

New insight into transmembrane topology of *Staphylococcus aureus* histidine kinase AgrC

Lina Wang [a,1], Chunshan Quan [b,c,*,1], Wen Xiong [b,c], Xiaojing Qu [b,c], Shengdi Fan [b,c], Wenzhong Hu [b,c]

[a] Dalian Institute of Chemical Physics, Chinese Academy of Sciences, 457 Zhong-shan Road, Dalian 116023, China
[b] Department of Life Science, Dalian Nationalities University, Economical and Technological Development Zone, Dalian 116600, China
[c] The State Ethnic Affairs Commission–Ministry of Education, Economical and Technological Development Zone, Dalian 116600, China

ARTICLE INFO

Article history:
Received 28 August 2013
Received in revised form 8 December 2013
Accepted 10 December 2013
Available online 17 December 2013

Keywords:
AgrC
Topology
GFP
SCAM
Staphylococcus aureus

ABSTRACT

Staphylococcus aureus accessory gene regulator (*agr*) locus controls the expression of virulence factors through a classical two-component signal transduction system that consists of a receptor histidine protein kinase AgrC and a cytoplasmic response regulator AgrA. An autoinducing peptide (AIP) encoded by *agr* locus activates AgrC, which transduces extracellular signals into the cytoplasm. Despite extensive investigations to identify AgrC–AIP interaction sites, precise signal recognition mechanisms remain unknown. This study aims to clarify the membrane topology of AgrC by applying the green fluorescent protein (GFP) fusion technique and the substituted cysteine accessibility method (SCAM). However, our findings were inconsistent with profile obtained previously by alkaline phosphatase. We report the topology of AgrC shows seven transmembrane segments, a periplasmic N-terminus, and a cytoplasmic C-terminus.

1. Introduction

Staphylococcus aureus is a versatile pathogenic bacterium that causes many acute and chronic infections throughout the world [1–3]. The pathogenicity of *S. aureus* primarily depends on a number of virulence factors, including cell wall-associated proteins involved in the attachment of the bacteria to host cells and protecting the bacteria against host defenses and secreted proteins to attack host cells and interfere with immune responses [4,5]. The expression of these virulence factors is primarily orchestrated by a quorum-sensing system encoded by the global regulatory locus, the accessory gene regulator (*agr*). The *agr* locus is known to contain two divergent transcripts known as RNAII and RNAIII, whose transcription is driven by the action of the P2 and P3 promoters, respectively. The RNAIII functions as a regulator that controls the expression of virulence factor genes, while the divergently transcribed RNAII is an operon containing four genes, *agrBDCA*, which encodes the core components of the quorum-sensing system [6–9]. In the *agr* operon, the proteins AgrB and AgrD are essential for production of the signal molecule, autoinducing peptide (AIP) [10,11], while AgrA and AgrC constitute a two-component system that is activated through an interaction of between AgrC and AIP. AgrC is a sensor kinase of the classic two-component signal transduction system. The N-terminal polytopic transmembrane sensor domain of AgrC interacts with AIP, while the C-terminal histidine kinase domain is a transmitter that is autophosphorylated at a conserved histidine upon stimulation by the signal molecule [12,13].

In previous studies, Geisinger et al. and Jensen et al. found that various amino acid residues may be important for AgrC–AIP recognition [14–16]. George Cisar et al. proposed that AgrC may function as a homodimer, but do not exclude the possibility of the existence of higher-order oligomers [17]. AgrC belongs to a typical member of the class 10 receptor-histidine protein kinase (HPK) [18]; however, the 3D structures of HPK_{10} kinases have not yet been resolved. Determination of the membrane topology model representing the number of transmembrane segments (TMSs) and their orientations is an important first step in understanding the structure/function relationships of a membrane protein. AgrC is predicted to consist of six to seven TMSs depending on the prediction algorithms used. The topology predictions vary, in particular for the N-terminal region of the protein which contains the sensory domain. Lina et al. reported that AgrC possesses five TMSs according to alkaline phosphatase (phoA) fusion studies [12]. Their results showed that amino acid residue 33 is outside, suggesting that the first predicted TMS and the N-terminus of AgrC are also outside. However, these hypotheses have not been examined in detail. Additionally, the second and third TMS positions have not yet been resolved. To further understand the functional mechanism of AgrC in signal transmission, it is necessary to determine the structural elements of the protein, such as orientation in the membrane and the number of TMSs.

* Corresponding author at: Department of Life Science, Dalian Nationalities University, Economical and Technological Development Zone, Dalian 116600, China. Tel.: +86 411 87656219; fax: +86 411 87644496.
E-mail addresses: wanglina.gucas@hotmail.com (L. Wang), mikyeken@dlnu.edu.cn (C. Quan), xiongwen-jan@hotmail.com (W. Xiong), qxj1229@hotmail.com (X. Qu), fsd@dlnu.edu.cn (S. Fan), hwz@dlnu.edu.cn (W. Hu).
[1] Equal contributions as first authors.

0005-2736/$ – see front matter © 2013 Elsevier B.V. All rights reserved.
http://dx.doi.org/10.1016/j.bbamem.2013.12.006

In this study, C-terminal and N-terminal fusions of AgrC to green fluorescent protein (GFP) were used. GFP only fluoresces when located in the cytoplasm of bacteria [19]. Thus, a model for the topology of TMSs and hydrophilic loops was accomplished by using reporter GFP fused to different regions of the membrane protein. However, these large fusions may have led to some altered membrane arrangements; therefore, we employed a mapping technique known as the substituted cysteine accessibility method (SCAM), which produces fewer structural perturbations [20–23]. GFP fusion experiments together with SCAM revealed a consistent model for AgrC topology. Our findings complement earlier studies of AgrC topology and, in combination with these prior results, we unambiguously establish a 7-TMS topological structure for AgrC.

2. Materials and methods

2.1. Construction of pAgrC–GFP and cysteine mutants of AgrC

Plasmids *pAgrC–GFP* were constructed using restriction-free cloning [24,25]. Cysteine mutants and the histidine mutant of AgrC were constructed by PCR using the QuickChange Site-Directed Mutagenesis Kit (Stratagene, La Jolla, CA, USA). All of the primers used in this study are listed in Supplementary Tables S1 and S2. Plasmid pET-28a-AgrC was used as a template. The integrity of all fusion constructs and site-directed mutagenesis was verified by nucleotide sequencing.

2.2. Cysteine labeling of AgrC

Escherichia coli C43(DE3) cells harboring pET-28a-AgrC vectors carrying the indicated mutation sites were induced with 0.1 mM isopropyl-β-D-1-thiogalactopyranoside (IPTG). Cells were washed twice and resuspended in ice-cold phosphate-buffered saline (PBS), pH 7.4. Cysteines were labeled with 100 μM or 500 μM 5-iodoacetamidofluorescein (5-IAF, Invitrogen, Carlsbad, CA, USA), which is a fluorescent membrane-impermeable thiol-reactive reagent. Iodoacetamides primarily react with sulfhydryl groups to form stable thioether bonds at physiological pH and at room temperature or below. Cells were incubated with 5-IAF for 30 min at room temperature and excess 5-IAF was quenched by adding 10 mM dithiothreitol (DTT). After incubation, cells were washed five times with PBS buffer pH 7.4, and disrupted by sonication. AgrC was purified using immobilized metal affinity chromatography (IMAC) and size exclusion chromatography (SEC) as described by Wang et al. [26]. Subsequently, samples purified were loaded onto a 12% SDS-polyacrylamide gel electrophoresis (SDS-PAGE). Following electrophoresis, in-gel fluorescence was recorded using the UVP GelDoc-It Imaging System (Upland, CA, USA).

2.3. Western blotting analysis

All the samples were resolved on standard 12% SDS-PAGE. Proteins were transferred to polyvinylidene difluoride membranes. The membranes were blocked with 5% dry milk in PBST (PBS containing 0.5% Tween 20, pH 7.4) for 3 h and probed for 2 h with a rabbit anti-His antibody (Sigma-Aldrich, St. Louis, MO, USA) at a dilution of 1:10,000 in PBST containing 5% dry milk. After five washes with PBST, membranes were incubated for 2 h on a shaker with Rabbit-anti-Mouse horseradish peroxidase (HRP)-conjugated secondary antibody (Sigma-Aldrich, St. Louis, MO, USA) in PBST at a 1:10,000 dilution. After five additional washes with PBST, the blots were developed with Amersham ECL Plus reagent (GE Health-care, Little Chalfont, UK) and exposed to autoradiography film.

2.4. GFP fluorescence

C43(DE3) cells harboring the indicated *pAgrC–GFP* plamids with various fusion points were induced using 0.1 mM IPTG at 20 °C for 24 h. Cells were washed once and resuspended in PBS, pH 7.0. Resuspended cells were crushed through a High Pressure Homogenizer (JN-3000 PLUS) at a pressure of 1000 bar at least three times at 4 °C. Lysed cells were subjected to centrifugate at 24,000 ×*g* for 20 min at 4 °C to remove unbroken cells and debris. The membranes were pelleted by ultracentrifugation at 300,000 ×*g* for 1 h and then resuspended in PBS. Fluorescence of the whole cells and cell membranes was measured with a fluorescence spectrophotometer (BioTek, Winooski, VT, USA) using an excitation wavelength of 485 nm and an emission wavelength of 510 nm. For each sample, the background fluorescence of the cells carrying the empty vector plasmid was subtracted. Experiments were performed in triplicate.

2.5. Autophosphorylation assays

The intrinsic kinase activity of single-cysteine-substituted AgrC mutants was measured by quantitating the amount of adenosine 5′-triphosphate (ATP) remaining in solution following a kinase reaction using Kinase-Glo Luminescent Kinase Assay Kit (Promega, Fitchburg, WI, USA). The assay was performed in 50 μL kinase reaction volume containing 200 μg AgrC mutants and 5 μM ATP in assay buffer consisting of 20 mM N-(2-hydroxyethyl)piperazine-N′-propanesulfonic acid (HEPES), pH 7.4, 10 mM $MgCl_2$, 0.5% N,N-dimethyldodecylamine N-oxide (LDAO) (w/v), and 1 mM DTT. In addition, a site specific mutation of the key histidine residue (H239N) of AgrC was included. Negative controls were reaction mixtures without protein kinase. The kinase reaction mixture was incubated for 15 min at 37 °C. Following incubation, 50 μL of ATP detection reagent was added to the assay plates. The assay plates were then incubated at 37 °C for 10 min, and the relative light unit (RLU) signal was measured using the Synergy 2 Multi-Mode Microplate Reader (BioTek, Winooski, VT, USA). The luminescent signal is correlated with the amount of ATP present and is inversely correlated with the amount of kinase activity.

3. Results

3.1. Prediction of AgrC topology model

Based on the published AgrC topology map (Fig. 1A) [12], the status of transmembrane helices I–III, and N-terminal location have not been resolved. In the absence of a three-dimensional structure for AgrC, we analyzed the transmembrane topology using various programs available through the internet. These programs included TMPred [27], TMHMM 2.0 [28], TOPCONS [29], TopPred II [30], SOSUI [31], and MEMSAT 2 [32,33]. Prediction performance during reassessment and consensus prediction were mainly based on three attributes: (1) the number of TMSs, (2) TMS-position, and (3) N-tail and C-tail locations (cytoplasm or periplasm) [34]. Supplementary Table S3 shows the overall prediction performance of each of the six selected TM prediction methods. By analyzing the prediction results, it is clear that there are six or seven potential TMSs in the N-terminal domain (Fig. 1B and C). Surprisingly, these prediction results were quite different from previously published topology maps [12,14,16]. We also found that the locations of the final four transmembrane helices were nearly identical among these prediction methods. However, the prediction analyses for the first two to three TMSs (residues 1–78) differed greatly.

3.2. Transmembrane topology of AgrC by GFP fusions

The predicted transmembrane topology of AgrC was confirmed by construction of AgrC–GFP and GFP–AgrC fusions at various points in the protein. PCR products of GFP with different primers were cloned into the pET-28a-AgrC vector to create a series of *agrC–gfp* and *gfp–agrC* fusion plasmids at the 12 sites indicated by the curves in Fig. 1C. A total of 12 fusion plasmids were generated (Supplementary Fig. S1). The whole-cell fluorescence intensity of each strain expressing the GFP fusion protein was measured (Fig. 2A). The location of the fusion

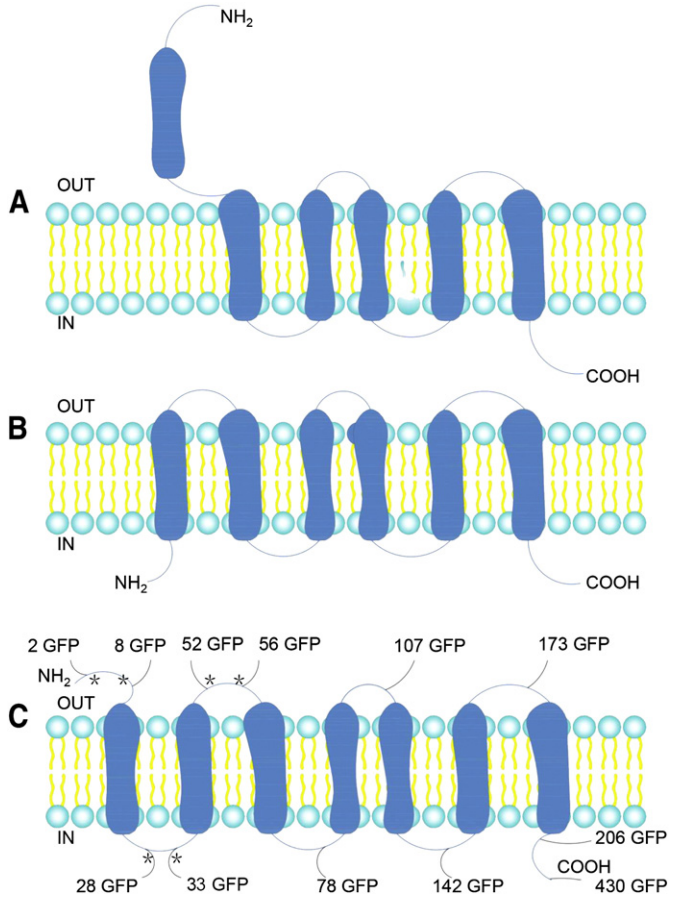

Fig. 1. Different AgrC membrane topology. (A) The topology map reported by Lina et al. based on phoA fusions. (B) AgrC topology as predicted by the topology analysis programs TMPred, TMHMM, and TopPred II. (C) AgrC topology as predicted by the topology analysis programs TOPCONS, SOSUI, and MEMSAT 2. Locations of the GFP fusion points are indicated. Asterisks indicate cysteine substitution resulting from site-directed mutagenesis.

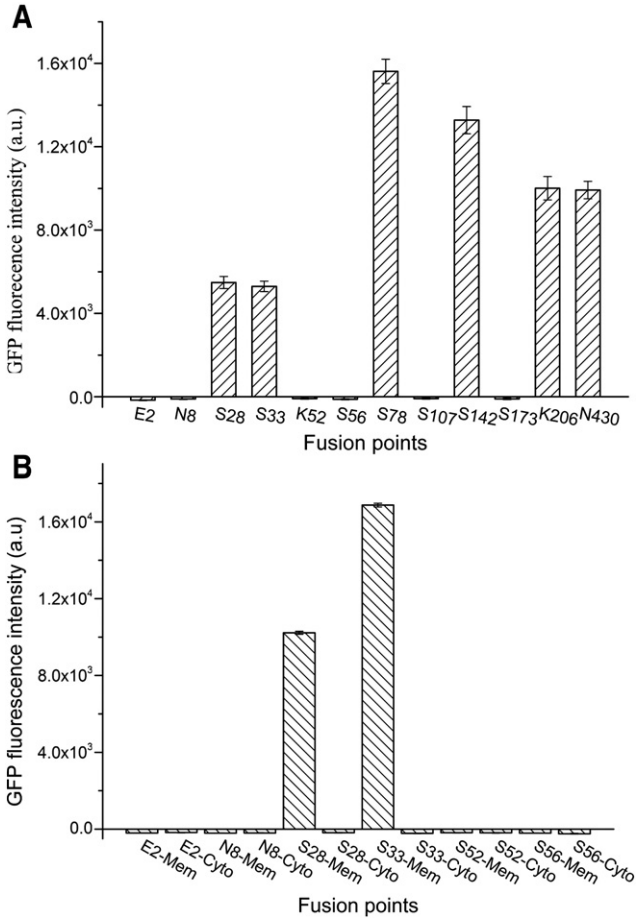

Fig. 2. Fluorescence analysis of cells expressing GFP–AgrC and AgrC–GFP fusion proteins. (A) Whole-cell fluorescence intensity from 200 μL cells overexpressing GFP–AgrC and AgrC–GFP fusion proteins. The average value of three measurements is shown. Numbers indicating the fusion sites refer to residue numbers in the sequence of AgrC. (B) Fluorescence analysis of cell membranes and the cytosol from cells expressing GFP–AgrC. Values represent the mean ± S.D. of three independent experiments. Numbers indicating the fusion sites refer to residue numbers in the sequence of AgrC. Mem: cell membranes; Cyto: cytosol.

point for each fusion protein was then assigned based on the GFP fluorescence intensity. GFP-positive indicates that the GFP portion, the fusion point of the protein, is in the cytoplasm, whereas GFP-negative indicates that the fusion point is in the periplasm. The fusions Glu-2, Asn-8, Lys-52, Ser-56, Ser-107, and Ser-173 failed to show any GFP fluorescence, suggesting that amino acid residues 2, 8, 52, 56, 107, and 173 were in the periplasm. The full-length AgrC–GFP fusion (Asn-430), amino acid residues Ser-28, Ser-33, Ser-78, Ser-142, and Lys-206 showed a strong fluorescence intensity, indicating that the C terminus of AgrC and amino acid residues 28, 33, 78, 142, and 206 were in the cytoplasm.

To confirm that the N-terminal GFP fusion proteins are integrated into the membrane and not mis-targeted to the cytosol, the cell membranes (membrane proteins) and the cytosol (soluble proteins) were separated by ultracentrifuge. Then the cell membranes containing membrane proteins were resuspended and washed three times with PBS buffer. Fluorescence of the same concentration of resuspended cell membranes and soluble proteins was measured with a fluorescence spectrophotometer. As shown in Fig. 2B, cell membranes of S28 and S33 fusions showed high fluorescence intensity and soluble proteins displayed no fluorescence, indicating that the N-terminal fusion proteins are integrated into the membrane and not mis-targeted to the cytosol. In addition, expression of the fusion proteins in C43(DE3) carrying the *agrC–gfp* or *gfp–agrC* fusion plasmid was evaluated by Western blotting of cell membranes. The molecular weight of all the fusion proteins was not consistent with the calculated molecular weight (Supplementary Fig. S2), which can be interpreted by the conservation of the structure of the GFP fraction [35].

The final four TMSs predicted by the models (Supplementary Table S3) were confirmed based on the GFP fluorescence of Ser-78, Ser-107, Ser-142, Ser-173 and K-206. The final four TMSs, located at residues 79–101, 110–132, 144–167, and 184–205, were evaluated. For amino acid residues 1–78, the results of prediction and the original AgrC topology map generated using PhoA fusions differed. The fusions Ser-28 and Ser-33 showed obvious fluorescence intensity, while the fusions Glu-2, Asn-8, and Ser-56 displayed no fluorescence, indicating that the first TMS contains 19 amino acid residues from Phe-9 to Ile-27 and the N-terminus is located in the periplasm. In contrast, Lina et al. previously reported that the first TMS is located outside of the cell membrane. The fusions Ser-33, Lys-52, Ser-56, and Ser-78 were used to establish the topological structure for TMS2: amino acid residues 35–51 and for TMS3: amino acid residues 57–72. The data was in agreement with the model (as shown in Fig. 1C).

3.3. Functional characterization of AgrC cysteine substitution

Cysteine substitutions between Ser6 and Ser56 in AgrC may affect the protein function to varying degrees. Therefore, the autokinase activity of cysteine mutants of AgrC was measured. Additionally, a site specific mutation of the key histidine residue (H239N) of AgrC was included

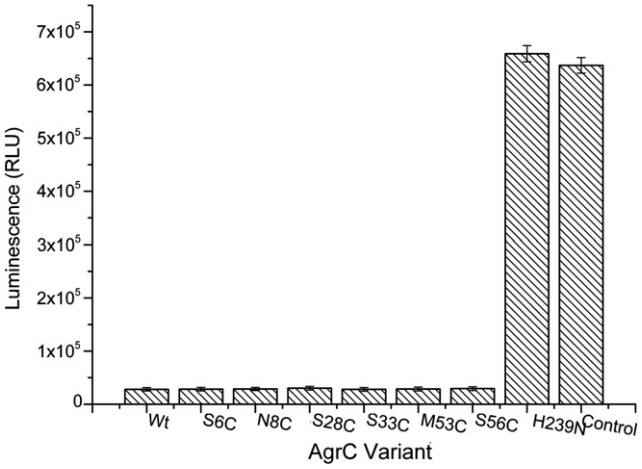

Fig. 3. Assessment of kinase activities of single-cysteine-substituted AgrC variants generated for topological studies. Data for each mutant are expressed as relative light unit (RLU). Values represent the mean ± S.D. of three independent experiments. $P < 0.001$.

to demonstrate that the kinase reaction is specific. Fig. 3 shows that cysteine substitutions had little effect on the kinase activity of AgrC and kinase reaction had high specificity. Next, TMSs I, II and III were determined by SCAM.

3.4. Determination of topology for TMSs by SCAM

First, SCAM studies were carried out using the native cysteine residues C84 and C371. Cells were treated with 5-IAF for extracellular cysteine labeling. Following purification, fluorescence of the 5-IAF labeling was not detected, suggesting that C84 and C371 were located either in the TMSs or in the cytoplasm (not shown). K-206 and N-430 are inside, which means that C371 was located in the cytoplasm. Since the fourth TMS includes amino acids 79–101, it is reasonable to determine that C84 is buried in the membrane. To further establish the topological structure of residues 1–78, six cysteine substitutions (S6C, N8C, S28C, S33C, M53C, and S56C) were engineered into AgrC. We targeted neutral residues whose substitutions would be less likely to interfere with AgrC structure. In presenting the SCAM findings on AgrC, the results from the experiments in *E. coli* are described (Fig. 4A). Residues near the N-terminus (S6C and N8C) reacted with both low and high concentrations of 5-IAF, indicating that this region is located outside of the cell. The next two residues (S28C and S33C) failed to label with 5-IAF, indicating these residues are located in the cytoplasm. The residues M53C and S56C all reacted with low and high concentrations of 5-IAF, suggesting an extracellular location.

Based on the results of the SCAM and GFP fusion analysis, we created a hypothetical AgrC topology map (Fig. 4B). Overall, the model depicts AgrC as containing seven TMSs. The six selected transmembrane analysis programs were used as a guide to assign the lengths of the individual TMS regions. Beginning with the N-terminus, we oriented AgrC residues 1–8 outside the cell. Next, we depicted residues 9–27 as a TMS (out-to-in) and residues 28–34 as an intracellular loop. SCAM findings are in agreement with GFP fusions. To orient the remaining AgrC protein topology, we relied on the striking extracellular labeling of residues M53C and S56C, coupled with the N-terminus GFP fusion of AgrC K52 and S56. Using these key features, residues 35–51 (in-to-out) and 57–72 (out-to-in) were depicted as TMSs as predicted by TOPCONS, SOSUI, and MEMSAT 2 analysis. Next, the residues from 52 to 56 were oriented as an extracellular loop based on the M53C and S56C.

Finally, we have oriented residues 79–101 (in-to-out), residues 110–132 (out-to-in), residues 144–167 (in-to-out), residues 184–205 (out-to-in) as transmembrane regions, 102–109, 168–183 as a short extracellular loop, and 206–end as an intracellular exposed tail. This representation was based on SCAM and GFP fusion results.

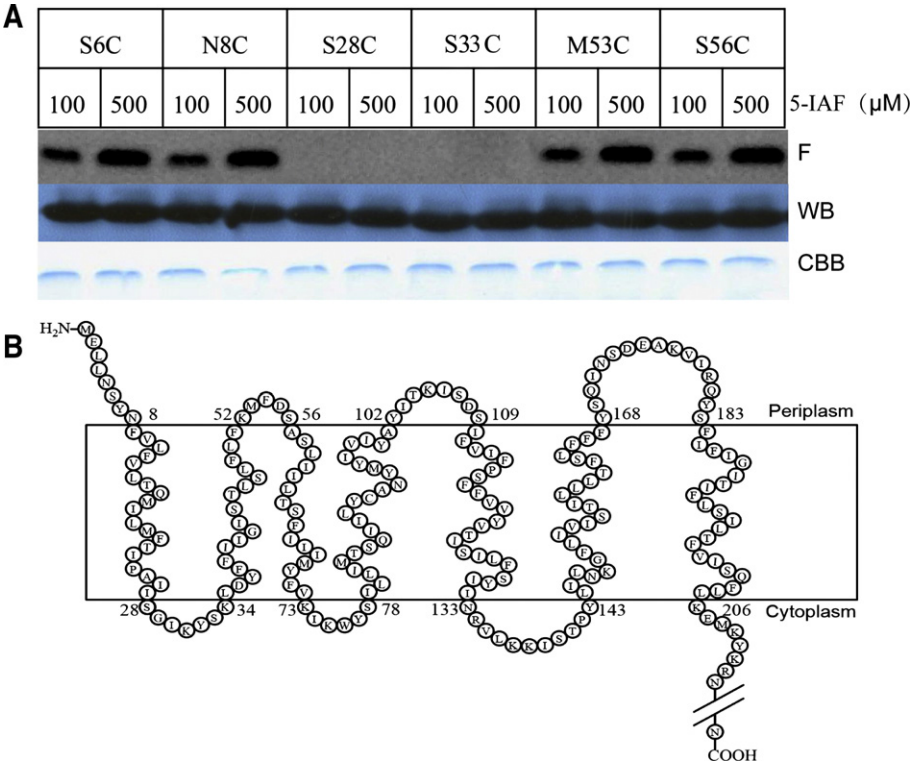

Fig. 4. Mapping AgrC topology in *E. coli* using SCAM. (A) Cells expressing the Cys variant of the full-length proteins as indicated were treated with 100 μM and 500 μM 5-IAF for 20 min. Following partial purification, the proteins were analyzed by SDS-PAGE (see the Materials and methods section). F, fluorescence image of the part of the gel containing the protein; WB, the same part of the gel was immunoblotted with anti-His-HRP to detect AgrC. CBB, same part of the gel was stained with Coomassie brilliant blue. (B) Proposed transmembrane topology of AgrC. The positions of the seven TMSs of the protein as predicted by prediction algorithms and as established based on GFP fusion and SCAM results are shown. Part of the cytoplasm is omitted.

4. Discussion

The *S. aureus* histidine kinase AgrC is well-recognized as a critical receptor protein of signal recognition and transmission with numerous studies focusing on AIP–AgrC interaction sites. In contrast, comparatively few reports have been conducted to determine the topology of AgrC. In this study, we utilized GFP fusion and SCAM to define membrane protein AgrC topology, which is useful for identifying the orientation, number, and size of TMSs.

The results of GFP fusions reveal the presence of seven TMSs, which agrees with the results of TOPCONS, SOSUI, and MEMSAT 2 analysis. Surprisingly, the result for the seven TMSs was quite different from the published topology maps (compare Fig. 1A, B, and C). Most notably, the N-terminus (residues 1–8) was oriented toward the outside of the cell and the residues 9–27 were adjusted as the first TMS (out-to-in), resulting in seven predicted TMSs rather than the reported five or six. GFP fusion technology has been widely used to determine the topology of integral membrane proteins, since the technology can rapidly and efficiently monitor the N-terminal or C-terminal of membrane protein overexpression in the periplasmic space or the cytoplasm. However, it has also suffered widespread criticism focusing on the use of truncated N-terminal fragments to determine the localization of internal sequence positions in the sequence [36], since the presence of the GFP at a protein N-terminus may lead to structural alterations.

As shown in Fig. 2A, after deletion of the first and first two TMSs at the N-terminus, the expression level of the membrane protein was improved due to reduction of the transmembrane helices. Generally, the more transmembrane domains, the more difficult it is to express membrane protein. Deletion of the first and first two TMSs at the N-terminus does not interfere with the topology, we thought the cause might be associated with the mechanism of membrane protein insertion. There are a lot of views about the mechanism of membrane protein insertion [37–40]. However, it's not known how an N-terminal GFP fusion can insert into the cell membrane.

To precisely determine AgrC topology, we further evaluate the AgrC membrane topology using SCAM. The advantage of SCAM is that protein structural integrity is maintained, which is very helpful for elucidating membrane topology questions. 5-IAF labeling of the residues (S6C, N8C, S28C, S33C, M53C, and S56C) at the cytoplasmic membrane border of TMSs I–III was very successful for defining the border at the residue level. Cysteine mutants showed full kinase activity (Fig. 3), further confirming that sufficient amounts of these mutants were correctly folded and targeted to the plasma membrane. SCAM, as a high-resolution and less invasive approach, provides a very accurate analysis of the residues in and around the membrane border. In future, this analysis can be combined with structural predictions or additional structural analysis, such X-ray crystallography or nuclear magnetic resonance, to provide an accurate topological map of membrane proteins.

Our interpretation of the GFP fusions and SCAM results led to the revision of the previously proposed AgrC topology, confirming that there are seven TMSs, with the N-terminus located on the outside of the cell, and C-terminus located inside of the cell (Fig. 4B). A new AgrC topology map was presented, which may facilitate ongoing efforts to understand AgrC function and signal transduction mechanisms. This is the first report of using the GFP fusion and SCAM to assess AgrC membrane topology. Finally, an accurate understanding of AgrC topology may be exploited in attempts to develop novel agents against virulence of *S. aureus* virulence.

Acknowledgements

This work was supported by the National Natural Science Foundation of China (grant No. 21272031 and grant No. 21172028), the Special Fund of the Central University (grant No. DC1210118), and the National Science and Technology Pillar Program during the 12th Five-year Plan Period (grant No. 2012BAD38B05).

Appendix A. Supplementary data

Supplementary data to this article can be found online at http://dx.doi.org/10.1016/j.bbamem.2013.12.006.

References

[1] D.J. Diekema, M.A. Pfaller, F.J. Schmitz, J. Smayevsky, J. Bell, R.N. Jones, M. Beach, Survey of infections due to *Staphylococcus* species: frequency of occurrence and antimicrobial susceptibility of isolates collected in the United States, Canada, Latin America, Europe, and the Western Pacific region for the SENTRY Antimicrobial Surveillance Program, 1997–1999, Clin. Infect. Dis. 32 (2001) S114–S132.
[2] F.D. Lowy, *Staphylococcus aureus* infections, N. Engl. J. Med. 339 (1998) 520–532.
[3] R.J. Gorwitz, D. Kruszon-Moran, S.K. McAllister, G. McQuillan, L.K. McDougal, G.E. Fosheim, B.J. Jensen, G. Killgore, F.C. Tenover, M.J. Kuehnert, Changes in the prevalence of nasal colonization with *Staphylococcus aureus* in the United States, 2001–2004, J. Infect. Dis. 197 (2008) 1226–1234.
[4] L. Janzon, S. Arvidson, The role of the delta-lysin gene (hld) in the regulation of virulence genes by the accessory gene regulator (agr) in *Staphylococcus aureus*, EMBO J. 9 (1990) 1391–1399.
[5] A.L. Cheung, A.S. Bayer, G. Zhang, H. Gresham, Y.Q. Xiong, Regulation of virulence determinants in vitro and in vivo in *Staphylococcus aureus*, FEMS Immunol. Med. Microbiol. 40 (2004) 1–9.
[6] R.P. Novick, S.J. Projan, J. Kornblum, H.F. Ross, G. Ji, B. Kreiswirth, F. Vandenesch, S. Moghazeh, The *agr* P2 operon: an autocatalytic sensory transduction system in *Staphylococcus aureus*, Mol. Gen. Genet. 248 (1995) 446–458.
[7] R.P. Novick, H.F. Ross, S.J. Projan, J. Kornblum, B. Kreiswirth, S. Moghazeh, Synthesis of staphylococcal virulence factors is controlled by a regulatory RNA molecule, EMBO J. 12 (1993) 3967–3975.
[8] Y. Benito, F.A. Kolb, P. Romby, G. Lina, J. Etienne, F. Vandenesch, Probing the structure of RNAIII, the *Staphylococcus aureus* agr regulatory RNA, and identification of the RNA domain involved in repression of protein A expression, RNA 6 (2000) 668–679.
[9] K. Tegmark, E. Morfeldt, S. Arvidson, Regulation of agr-dependent virulence genes in *Staphylococcus aureus* by RNAIII from coagulase-negative staphylococci, J. Bacteriol. 180 (1998) 3181–3186.
[10] G. Ji, R. Beavis, R.P. Novick, Cell density control of staphylococcal virulence mediated by an octapeptide pheromone, Proc. Natl. Acad. Sci. U. S. A. 92 (1995) 12055–12059.
[11] G. Ji, R. Beavis, R.P. Novick, Bacterial interference caused by autoinducing peptide variants, Science 276 (1997) 2027–2030.
[12] G. Lina, S. Jarraud, G. Ji, T. Greenland, A. Pedraza, J. Etienne, R.P. Novick, F. Vandenesch, Transmembrane topology and histidine protein kinase activity of AgrC, the agr signal receptor in *Staphylococcus aureus*, Mol. Microbiol. 28 (1998) 655–662.
[13] G.J. Lyon, J. Wright, A. Christopoulos, R.P. Novick, T.W. Muir, Reversible and specific extracellular antagonism of receptor-histidine kinase signaling, J. Biol. Chem. 277 (2002) 6247–6253.
[14] E. Geisinger, E.A. George, T.W. Muir, R.P. Novick, Identification of ligand specificity determinants in AgrC, the *Staphylococcus aureus* quorum-sensing receptor, J. Biol. Chem. 283 (2008) 8930–8938.
[15] E. Geisinger, T.W. Muir, R.P. Novick, agr receptor mutants reveal distinct modes of inhibition by staphylococcal autoinducing peptides, Proc. Natl. Acad. Sci. U. S. A. 106 (2009) 1216–1221.
[16] R.O. Jensen, K. Winzer, S.R. Clarke, W.C. Chan, P. Williams, Differential recognition of *Staphylococcus aureus* quorum-sensing signals depends on both extracellular loops 1 and 2 of the transmembrane sensor AgrC, J. Mol. Biol. 381 (2008) 300–309.
[17] E.A. George Cisar, E. Geisinger, T.W. Muir, R.P. Novick, Symmetric signalling within asymmetric dimers of the *Staphylococcus aureus* receptor histidine kinase AgrC, Mol. Microbiol. 74 (2009) 44–57.
[18] E.A. George Cisar, E. Geisinger, T.W. Muir, R.P. Novick, T.W. Grebe, J.B. Stock, The histidine protein kinase superfamily, Adv. Microb. Physiol. 41 (1999) 139–227.
[19] D.O. Daley, M. Rapp, E. Granseth, K. Melén, D. Drew, G. von Heijne, Global topology analysis of the *Escherichia coli* inner membrane proteome, Science 308 (2005) 1321–1323.
[20] M. Thoendel, A.R. Horswill, Random mutagenesis and topology analysis of the autoinducing peptide biosynthesis proteins in *Staphylococcus aureus*, Mol. Microbiol. 87 (2013) 318–337.
[21] A.D. Rusden, D.P. Stephenson, N.K. Verma, Topological investigation of glucosyltransferase V in *Shigella flexneri* using the substituted cysteine accessibility method, Biochemistry 52 (2013) 2655–2661.
[22] M. Bogdanov, W. Zhang, J. Xie, W. Dowhan, Transmembrane protein topology mapping by the substituted cysteine accessibility method (SCAM(TM)): application to lipid-specific membrane protein topogenesis, Methods 36 (2005) 148–171.
[23] Q. Zhu, J.R. Casey, Topology of transmembrane proteins by scanning cysteine accessibility mutagenesis methodology, Methods 41 (2007) 439–450.
[24] F. Van Den Ent, J. Löwe, RF cloning: a restriction-free method for inserting target genes into plasmids, J. Biochem. Biophys. Methods 67 (2006) 67–74.
[25] T. Unger, Y. Jacobovitch, A. Dantes, R. Bernheim, Y. Peleg, Applications of the restriction free (RF) cloning procedure for molecular manipulations and protein expression, J. Struct. Biol. 172 (2010) 34–44.
[26] L.N. Wang, C.S. Quan, B.Q. Liu, Y.B. Xu, W. Xiong, S.D. Fan, Green fluorescent protein (GFP)-based overexpression screening and characterization of AgrC, a receptor protein of quorum sensing in *Staphylococcus aureus*, Int. J. Mol. Sci. 14 (2013) 18470–18487.

[27] K. Hofmann, W. Stoffel, TMbase—a database of membrane spanning proteins segments, Biol. Chem. Hoppe Seyler 347 (1993) 166.
[28] A. Krogh, B. Larsson, G. von Heijne, E.L. Sonnhammer, Predicting transmembrane protein topology with a hidden Markov model: application to complete genomes, J. Mol. Biol. 305 (2001) 567–580.
[29] A. Bernsel, H. Viklund, A. Hennerdal, A. Elofsson, TOPCONS: consensus prediction of membrane protein topology, Nucleic Acids Res. 37 (2009) W465–W468.
[30] M.G. Claros, G. von Heijne, TopPred II: an improved software for membrane protein structure predictions, Comput. Appl. Biosci. 10 (1994) 685–686.
[31] T. Hirokawa, S. Boon-Chieng, S. Mitaku, SOSUI: classification and secondary structure prediction system for membrane proteins, Bioinformatics 14 (1998) 378–379.
[32] D.T. Jones, W.R. Taylor, J.M. Thornton, A model recognition approach to the prediction of all helical membrane protein structure and topology, Biochemistry 33 (1994) 3038–3049.
[33] L.J. McGuffin, K. Bryson, D.T. Jones, The PSIPRED protein structure prediction server, Bioinformatics 16 (2000) 404–405.
[34] M. Ikeda, M. Arai, D.M. Lao, T. Shimizu, Transmembrane topology prediction methods: a reassessment and improvement by a consensus method using a dataset of experimentally characterized transmembrane topologies, In Silico Biol. 2 (2002) 19–33.
[35] E.R. Geertsma, M.D. Groeneveld, J. Slotboom, Quality control of overexpressed membrane proteins, Proc. Natl. Acad. Sci. U. S. A. 105 (2008) 5722–5727.
[36] R. Ter Horst, J.S. Lolkema, Rapid screening of membrane topology of secondary transport proteins, Biochim. Biophys. Acta 1798 (2010) 672–680.
[37] S.H. White, G. von Heijne, The machinery of membrane protein assembly, Curr. Opin. Struct. Biol. 14 (2004) 397–404.
[38] V. Goder, T. Junne, M. Spiess, Sec61p contributes to signal sequence orientation according to the positive-inside rule, Mol. Biol. Cell 15 (2004) 1470–1478.
[39] T. Hessa, H. Kim, K. Bihlmaier, C. Lundin, J. Boekel, H. Andersson, I. Nilsson, S.H. White, G. von Heijne, Recognition of transmembrane helices by the endoplasmic reticulum translocon, Nature 433 (2005) 377–381.
[40] W. Dowhan, M. Bogdanov, Lipid-dependent membrane protein topogenesis, Annu. Rev. Biochem. 78 (2009) 515–540.